JOC Article
pubs.acs.org/joc

Single-Hole Hollow Nanospheres from Enantioselective Self-Assembly of Chiral AIE Carboxylic Acid and Amine

Dong-Mi Li and Yan-Song Zheng*

Department of Chemistry, Huazhong University of Science and Technology, Wuhan 430074, P.R. China

zyansong@hotmail.com

Received November 6, 2010

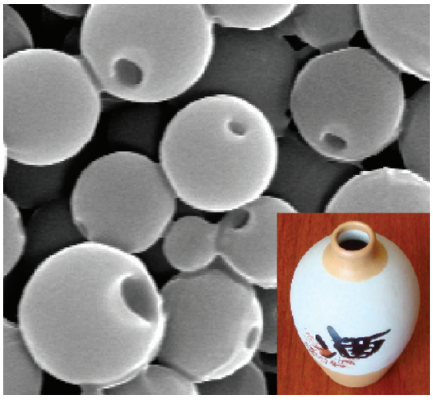

Phenylacrylonitrile tartaric acids have been found to enantioselectively self-assemble with an enantiomer of a chiral amine to form either nanofibers or nanospheres that exhibit aggregation-induced emission (AIE). The nanofibers exhibited stronger emission intensity and longer wavelengths of absorption and emission than the nanospheres because of increased $\pi-\pi$ conjugation, an effect previously unseen in AIE. When the solvent consists of a mixture of water and THF rather than water and ethanol, the resultant nanospheres have holes. The holes are the result of the dissolution of defects and a decrease in the bending energy. This is in contrast to hole formation from solvents flowing out of the nanospheres, as previously seen. Through control of the water/THF ratio, the size of the holes in the nanospheres can be tuned. Nanospheres with a single hole displayed both higher uptake capacity and larger release speed of the drug naproxen than closed nanospheres. The ability to adjust fluorescent properties of AIE molecules through the preparation of organic single-hole hollow nanospheres has also been investigated along with the implications of the AIE mechanism.

Introduction

Hollow nanospheres are attracting increasing interest as catalyst carriers, drug capsules, gas storage, pollutant removers, and cell imitators among others. These hollow spheres are closed, which makes it hard to encapsulate and release the guest molecules. In contrast most containers used in daily life, such as jam jars, milk bottles, and coffee cups have a hole for rapidly introducing and removing the contents. For example, the hydrogenation of ethylene catalyzed by platinum nanoparticles encapsulated in hollow spheres of CoO is 4 times slower than the platinum nanoparticles supported on SiO_2 which is because the reactants and products must diffuse through the closed shell.[1] Porous hollow nanospheres would appear to be a solution to this problem. Inorganic materials have used to produce porous hollow nanospheres made of carbon,[2] silica,[3] metal oxide,[4] sulfide,[5] nitride,[6] and phosphate.[7] A hollow aluminosilicate sphere with holes has

(1) Yin, Y.; Rioux, R. M.; Erdonmez, C. K.; Hughes, S.; Somorjai, G. A.; Alivisatos, A. P. *Science* **2004**, *304*, 711–714.

(2) (a) Yoon, S. B.; Sohn, K.; Kim, J. Y.; Shin, C.-H.; Yu, J.-S.; Hyeon, T. *Adv. Mater.* **2002**, *14* (1), 19–21. (b) Ma, L. J. J.; Zhao, C.; Wei, W.; Ji, L.; Wang, X.; Yang, M.; Lu, Y.; Yang, Z. *Chem. Commun.* **2006**, 1206–1208.

(3) (a) Suh, W. H.; Suslick, K. S. *J. Am. Chem. Soc.* **2005**, *127*, 12007–12010. (b) Li, L.; Choo, E. S. G.; Tang, X.; Ding, J.; Xue, J. *Chem. Commun.* **2009**, 938–940.

(4) (a) Liu, J.; Xue, D. *Adv. Mater.* **2008**, *20*, 2622–2627. (b) Shen, Z.-R.; Wang, J.-G.; Sun, P.-C.; Ding, D.-T.; Chen, T.-H. *Chem. Commun.* **2009**, 1742–1744.

Published on Web 01/18/2011 DOI: 10.1021/jo102206h

SCHEME 1. Structure of Phenylacrylonitrile Tartaric Acids 1−6, Amines 7−9, and Naproxen 10

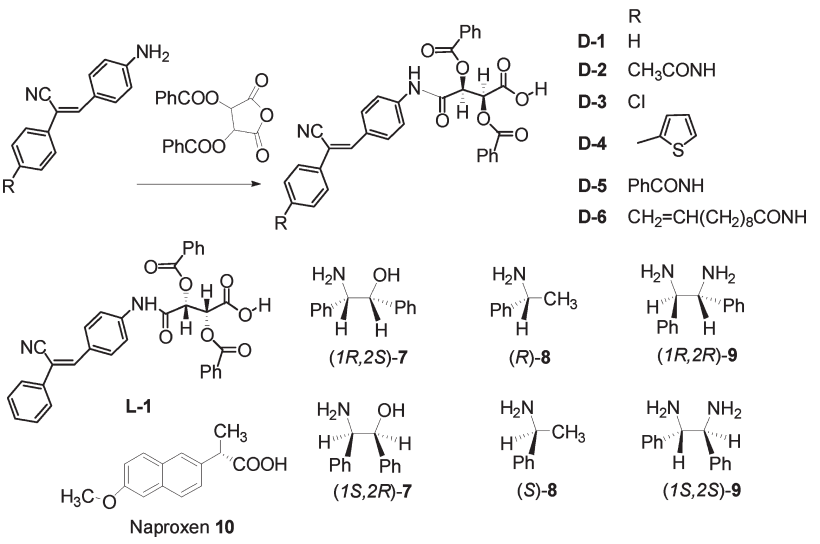

encapsulated *Discosoma* coral proteins which was not possible by a closed nanosphere.[8] Making these porous hollow nanospheres from organic materials would be advantageous for some applications such as drug delivery because of increased compatibility with the living body. However, there has been very little research on these kinds of organic nanomaterials. Porous hollow spheres based on organic polymers have been documented.[9−11] Hollow polymer spheres with a hole have been shown to adsorb more TNT explosives,[10] encapsulate bovine serum albumin,[9] and even accommodate iron oxide nanoparticles.[9] Therefore, more methods for the preparation of hollow organic spheres need to be developed.

Although the self-assembly of organic small molecules is one of the most convenient methods for the preparation of organic micro/nanomaterials, the fabrication of porous hollow nanospheres by this method are rare.[12] Recently, it has been reported that U-like porphyrin−Zn(II) complexes,[12a] V-like benziporphodimethene−Zn(II) complexes,[12b] dicyanomethylene-containing oligophenylenevinylene[12c] and dendritic peptides composed of palmitoyl tryptophan[12d] can self-assemble into hollow micro/nanospheres with holes on their surfaces, in addition to dumbbell-shaped nonionic amphiphiles[12e] which can form a capsule structure with mesh-like nanopores on its shell. Like the single hole in single-hole hollow nanospheres based on polymer, the holes in the surfaces of these hollow spheres are formed by the outflow of solvent included in the spheres. Research into their use as drug carriers has not been reported.

The chirality of organic small molecules has been exploited in the formation of nanomaterials[13] and can be used to tune their shape and size.[14] However, no work has yet related the effect of the molecular chirality on the properties of the organic micro/nano materials. Moreover, molecular chirality has not been used to prepare hollow nanospheres with holes. Here, we have prepared chiral phenylacrylonitrile tartaric acids, which exhibit aggregation-induced emission (AIE) and have investigated how the chirality controls the AIE. The mechanism for the formation of the hole on the surface of the spheres is also discussed.

Results and Discussion

Chiral compounds **1**−**6** (Scheme 1) bearing an optically pure tartaric acid group are a new class of molecules which exhibit aggregation-induced emission (AIE).[15,16] At the correct ratio of water to ethanol, D-**1** or L-**1** can induce the aggregation of just one enantiomer with a number of chiral amines. This causes a huge difference in the fluorescence intensity between enantiomers.[16] When the volume ratio of water and ethanol was increased to 9:1, both enantiomers of chiral amine **7** displayed aggregation with D-**1**, but the morphologies of the aggregates were different. FE-SEM revealed that aggregates made of D-**1** and (1*S*,2*R*)-**7** were made of nanofibers with a length of about 50 μm and a width of about 200 nm. But the aggregates of D-**1** and (1*R*,2*S*)-**7** were composed of round

(5) Fischer, C.-H.; Muffler, H.-J.; Ba1r, M.; Kropp, T.; Scho1nmann, A.; Fiechter, S.; Barbar, G.; Lux-Steiner, M. C. *J. Phys. Chem. B* **2003**, *107*, 7516–7521.
(6) Bang., J. H.; Suslick, K. S. *Adv. Mater.* **2009**, *21*, 1–5.
(7) Chen, C.; Chen, W.; Lu, J.; Chu, D.; Huo, Z.; Peng, Q.; Li, Y. *Angew. Chem., Int. Ed.* **2009**, *48*, 1–5.
(8) Shiomi, T.; Tsunoda, T.; Kawai, A.; Matsuura, S.; Mizukami, F.; Sakaguchi, K. *Small* **2009**, *5* (1), 67–71.
(9) Im, S. H.; Jeong, U.; Xia, Y. *Nat. Mater.* **2005**, *4*, 671–675.
(10) Guan, G.; Zhang, Z.; Wang, Z.; Liu, B.; Gao, D.; Xie, C. *Adv. Mater.* **2007**, *19*, 2370–2374.
(11) Chen, Y.; Qian, Z.; Zhang, Z. *Chem. Lett.* **2007**, *36* (7), 944–945.
(12) (a) Huang, C.; Wen, L.; Liu, H.; Li, Y.; Liu, X.; Yuan, M.; Zhai, J.; Jiang, L.; Zhu, D. *Adv. Mater.* **2009**, *21*, 1721–1725. (b) Huang, C.; Li, Y.; Yang, J.; Cheng, N.; Liu, H.; Li, Y. *Chem. Commun.* **2010**, *46*, 3161–3163. (c) Ghosh, S.; Verma, S. *Tetrahedron* **2008**, *64*, 6202–6208. (d) Xu, J.; Liu, X.; Lv, J.; Zhu, M.; Huang, C.; Zhou, W.; Yin, X.; Liu, H.; Li, Y.; Ye, J. *Langmuir* **2008**, *24*, 4231–4237. (e) Kim, J.-K.; Lee, E.; Lim, Y.; Lee, M. *Angew. Chem., Int. Ed.* **2008**, *47*, 1–5.
(13) (a) Brizard, A.; Oda, R.; Huc, I. *Top. Curr. Chem.* **2005**, *256*, 167–218. (b) Shimizu, T.; Masuda, M.; Minamikawa, H. *Chem. Rev.* **2005**, *105*, 1401–1443. (c) Zhang, J.; Albelda, M. T.; Liu, Y.; Canary, J. W. *Chirality* **2005**, *17*, 404–420. (d) Meurig, T. J.; Robert, R. *Acc. Chem. Res.* **2008**, *41*, 708–720. (e) de Loose, M.; van Esch, J.; Kellogg, R. M.; Feringa, B. L. *Angew. Chem., Int. Ed.* **2001**, *40*, 623–616.
(14) (a) Nandi, N.; Vollhardt, D. *Chem. Rev.* **2003**, *103*, 4033–4075. (b) Oda, R.; Huc, I.; Schmutz, M.; Candau, S. J.; MacKitosh, F. C. *Nature* **1999**, *399*, 566–569. (c) Messmore, B. W.; Sukerkar, P. A.; Stupp, S. I. *J. Am. Chem. Soc.* **2005**, *127*, 7992–7993. (d) Hirst, A. R.; Smith, D. K.; Feiters, M. C.; Geurts, H. P. M. *Chem.—Eur. J.* **2004**, *10*, 5901–5910.
(15) (a) Luo, J.; Xie, Z.; Lam, J. W. Y.; Cheng, L.; Chen, H.; Qiu, C.; Kwok, H. S.; Zhan, X.; Liu, Y.; Zhu, D.; Tang, B. Z. *Chem. Commun.* **2001**, 1740–1741. (b) Liu, L.; Zhang, G.; Xiang, J.; Zhang, D.; Zhu, D. *Org. Lett.* **2008**, *10*, 4581–4584.
(16) Zheng, Y.-S.; Hu, Y.-J. *J. Org. Chem.* **2009**, *74*, 5660–5663.

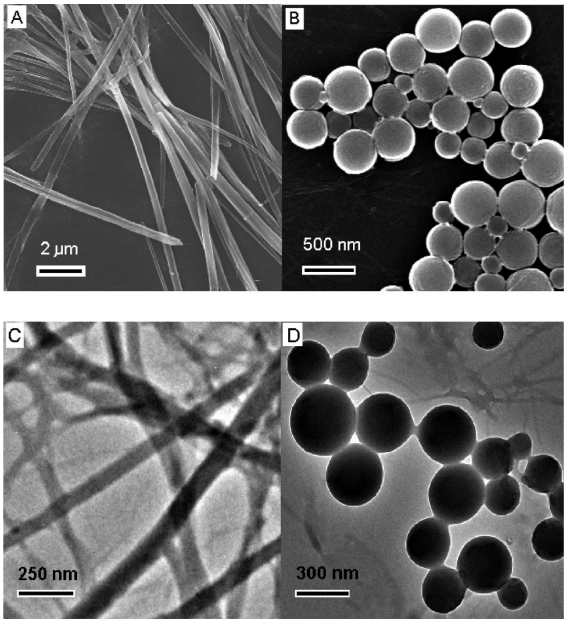

FIGURE 1. (A) FE-SEM image of mixture of D-**1** and (1*S*,2*R*)-**7** ; (B) FE-SEM image of D-**1** and (1*R*,2*S*)-**7**; (C) TEM image of D-**1** and (1*S*,2*R*)-**7**; (D) TEM images of D-**1** and (1*R*,2*S*)-**7**. [**1**] = [**7**] = 1.0×10^{-3} M in a mixed solvent of water and ethanol, v/v 9:1, mixing **1** and **7**.

TABLE 1. Enantioselective Morphology[a] and Quantum Yield (Φ_f %)[b]

	(1*R*,2*S*)-**7**	(1*S*,2*R*)-**7**	(*R*)-**8**	(*S*)-**8**
D-**1**	spheres	fibers	spheres	fibers
Φ_f %	0.43	25.0	2.76	5.96
D-**2**	spheres	fibers	fibers	spheres
Φ_f %	0.98	3.69	0.52	0.10
D-**3**	fibers	spheres	fibers	spheres
Φ_f %	3.10	0.43	2.80	0.30

[a]The concentrations of all reagents 1.0×10^{-3} M in a mixed solvent of water and ethanol, v/v 9:1, measured by FE-SEM. [b]Measured using quinine bisulfate in 1 N H_2SO_4 as the standard.

nanospheres with a diameter of 100−500 nm (Figure 1, A and B). TEM images confirmed the result observed by FE-SEM (Figure 1, C and D). As expected, if L-**1** was reacted with the amine, the mixture of L-**1** and (1*R*,2*S*)-**7** led to nanofibers, but L-**1** and (1*S*,2*R*)-**7** resulted in nanospheres, indicating that the shape difference of the aggregates was initiated by chiral recognition. In addition, the powder XRD pattern of dry solid obtained by filtering the suspension of D-**1** and (1*S*,2*R*)-**7** exhibited four peaks at low angles corresponding to *d*-spacing of 2.6, 1.5, 1.3, and 0.97 nm. However, the powder XRD pattern of D-**1** and (1*R*,2*S*)-**7** showed no peaks (Figures S21−S22, Supporting Information [SI]). This indicates that nanofibers have an orderly layered structure, which is accordance with the fact that the linear objects are anisotropic to a greater extent than spherical ones.

Mixing the optically pure acids D-**2** and D-**3** with the two enantiomers of the amine **7** also afforded aggregates with different morphologies. Similarly, D-**1**, D-**2**, or D-**3** reacts with the two enantiomers of the amine **8** to produce spherical and fiber aggregates, depending on the chirality. These results are summarized in Table 1. The fluorescence emission of the fiber aggregates is stronger much than that of the spherical aggregates. As shown in Table 1, the quantum yields Φ_f,

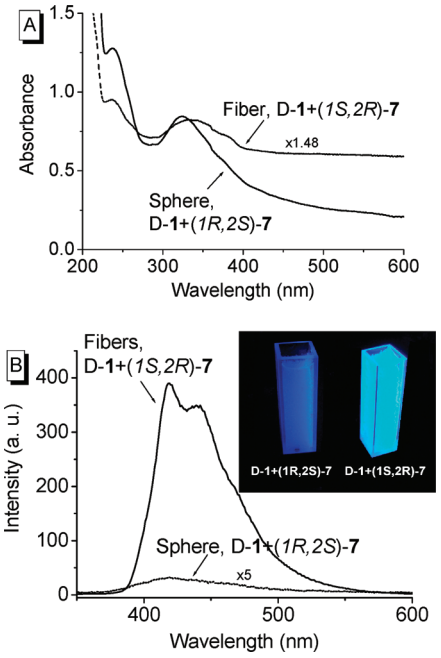

FIGURE 2. Absorption (A) and emission (B) spectra of a mixture of D-**1** and enantiomers of **7** in a mixed solvent of water and ethanol (v/v 9:1).

measured using quinine bisulfate in 1 N H_2SO_4 as the standard, are between 2 and 58 times greater in the nanofibers. Moreover, the peak wavelength λ_{max} of the absorption and emission of fiber aggregations occurs at longer wavelengths. For example, the λ_{max} of the nanofibers from the mixture of D-**1** and (1*S*,2*R*)-**7** was 20 nm (346 nm vs 326 nm) longer than that of the nanospheres formed by the interaction of D-**1** and (1*R*,2*S*)-**7**. The emission of the nanofibers also appeared at a wavelength that was 23 nm (443 nm vs 420 nm) longer than that of nanospheres (Figure 2). Irradiated under a portable 365 nm UV lamp, a suspension of D-**1** and (1*S*,2*R*)-**7** in water and ethanol (v/v 9:1) emitted strong green light, but D-**1** and (1*R*,2*S*)-**7** had a weak blue fluorescence (inset in Figure 2B).

Although chirality has been seen to affect self-assembly, examples of different chirality resulting in different aggregate morphology are very rare.[14] These differences in aggregate morphology leading to different emission properties have not been reported, to the best of our knowledge. The aggregation of **1**−**3** with both (1*R*,2*R*)-**9** and (1*S*,2*S*)-**9** only afforded round nanospheres with a diameter of 200−500 nm in the mixed solvent of water and ethanol (v/v 9:1).

Compound **4** has an additional conjugated thiophene group and emits more strongly at a longer wavelength than **1** when aggregated. Because of insolubility in ethanol, the aggregation of **4** with amines was carried out in a mixture of water and THF (v/v 90:10) instead of ethanol. When 1.8 mL of water was added to the solution of D-**4** (0.01 M) and **7** (0.01 M) in 0.2 mL of THF without stirring, the resultant aggregates of D-**4** and (1*S*,2*R*)-**7** were primarily nanofibers with a small amount of nanospheres, and D-**4** and (1*R*,2*S*)-**7** gave nanospheres with a few nanofibers, as observed in the FE-SEM images. D-**4** and (1*R*,2*R*)-**9** gave nanospheres with very few nanofibers, but D-**4** and (1*S*,2*S*)-**9** yielded nanorods composed of nanospheres connected to each other (Figure 3, A and B). Similar to the results in water and ethanol, the

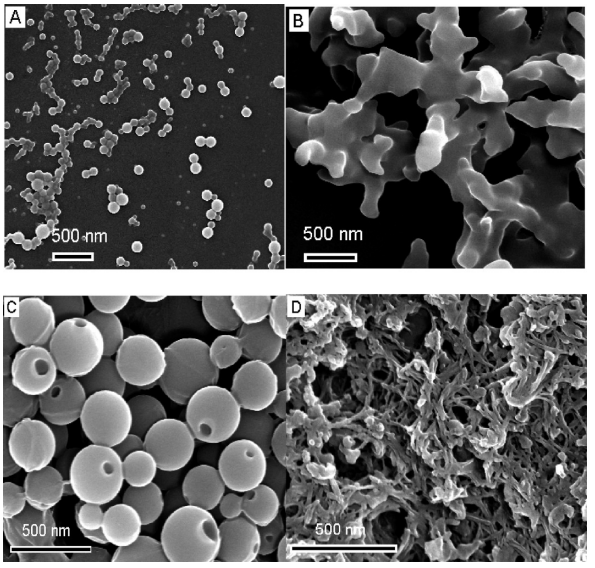

FIGURE 3. (A) FE-SEM image of mixture of D-**4** and (1*R*,2*R*)-**9** under no stirring; (B) FE-SEM image of mixture of D-**4** and (1*S*,2*S*)-**9** under no stirring; (C) FE-SEM image of mixture of D-**4** and (1*R*,2*R*)-**9** under stirring; (D) FE-SEM image of mixture of D-**4** and (1*S*,2*S*)-**9** under stirring; [**4**] = [**9**] = 1.0×10^{-3} M in a mixed solvent of water and THF, v/v 90:10.

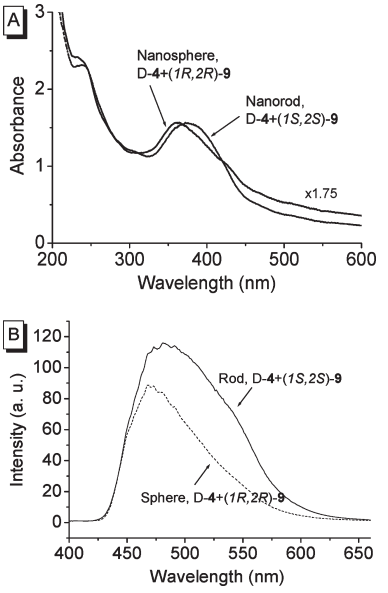

FIGURE 4. Absorption and emission spectra of mixture of D-**4** and enantiomers of **9**. (A) Absorption spectra; (B) emission spectra, λ_{ex} = 360 nm, ex/em slits = 3/3 nm. [**4**] = [**9**] = 1.0×10^{-3} M in a mixed solvent of water and THF (v/v 9:1).

suspension of nanofibers in water and THF had a stronger emission and longer absorption and emission λ_{max} than the nanospheres. As shown in Figure 4, the nanorod suspension of D-**4** and (1*S*,2*S*)-**9** in water and THF (v/v 90:10) had a larger absorption λ_{max} than that of the nanospheres of D-**2** and (1*R*,2*R*)-**9** (385 nm vs 365 nm). The emission λ_{max} of the nanorods also appeared at a wavelength that was 15 nm (486 nm vs 471 nm) longer than that of the nanospheres, and had a more intense emission.

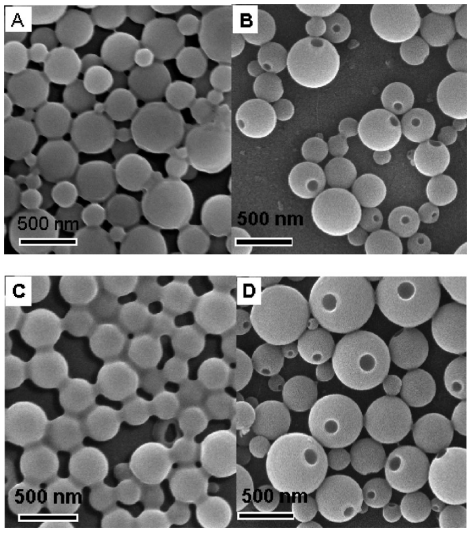

FIGURE 5. FE-SEM images of mixture of (A) D-**1** and (1*R*,2*R*)-**9** under no stirring; (B) D-**1** and (1*R*,2*R*)-**9** under stirring; (C) D-**2** and (1*R*,2*R*)-**9** under no stirring; (D) D-**2** and (1*R*,2*R*)-**9** under stirring in a mixed solvent of water and THF, v/v 95:5 (concentration of all compounds 1.0×10^{-3} M).

Unexpectedly, when the water was slowly added into the solution in THF while stirring to give a volume ratio of H_2O/THF, 90:10, the resultant aggregates of the mixture of D-**4** and (1*R*,2*R*)-**9** were nanospheres with a hole in their surfaces. As shown by FE-SEM image in Figure 3C, the nanospheres had diameters ranging from 150 to 800 nm and the holes in the surface were 20−150 nm in diameter. Under the same conditions, the nanorod aggregates of D-**4** and (1*S*,2*S*)-**9** had smaller diameters than those without stirring. It is noted that the minor nanospheres retained among the nanorods also bear a hole in the surface (Figure 3D).

When water was slowly added into the solution of other chiral AIE acids such as D-**1**, D-**2**, D-**3**, or D-**5** with (1*R*,2*R*)-**9** in THF under stirring, the resultant aggregates were nanospheres with a hole. Without stirring, only closed nanospheres were obtained. As shown in Figure 5A, rapidly adding the water to the solution of D-**1** and (1*R*,2*R*)-**9** in THF (volume ratio H_2O/THF, 95:5), gave nanospheres with diameters from 100 to 500 nm. When water was added slowly to the same solution with stirring, the resultant aggregates were single-hole nanospheres (Figure 5B). The nanospheres had diameters from 150 to 500 nm, and the holes in the surface had diameters from 30 to 100 nm. The mixture of D-**2**, D-**3**, or D-**5** with (1*R*,2*R*)-**9** in water and THF also displayed the same pattern as D-**1** with (1*R*,2*R*)-**9**. Without stirring, the aggregates were closed nanospheres, but under stirring, the aggregates were single-hole nanospheres (Figure 5, C and D; Figure S23, SI). Using other amines, such as (1*S*,2*S*)-**9**, enantiomers of **7** and **8**, the same results were also obtained.

Compound **6**, bearing a long-chain 10-undecenamide group, gave single-hole nanospheres more easily than the other acids. As shown in Figure 6, A and B, upon adding water, solutions of D-**6** and (1*R*,2*R*)-**9** in THF gave nanospheres with a single hole formed whether the solution was stirred or not. Moreover, compared with the single-hole nanospheres formed from D-**1**−D-**5**, the diameter of the hole (50−300 nm) was 3 times larger, while the size of the nanospheres (diameter of 120−700 nm) changed very little. Using (1*S*,2*S*)-**9** as the base, D-**6**

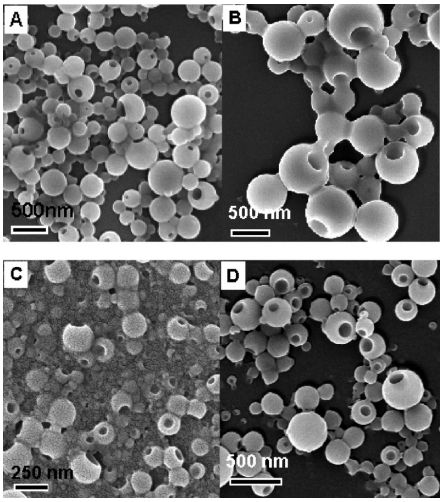

FIGURE 6. FE-SEM images of suspension of (A) D-**6** and (1*R*,2*R*)-**9** under no stirring; (B) D-**6** and (1*R*,2*R*)-**9** under stirring; (C) D-**6** itself without amine under no stirring; (D) D-**6** and (1*R*,2*R*)-**9** under no stirring and standing for a month in a mixed solvent of water and THF, v/v 95:5 (concentration of all compounds is 1.0×10^{-3} M).

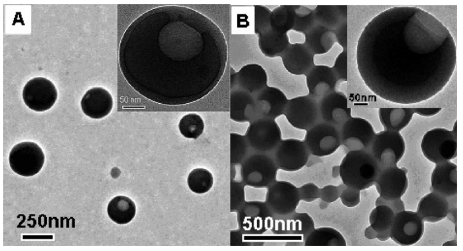

FIGURE 7. TEM images of mixture of (A) D-**1** and (1*R*,2*R*)-**9** under stirring; (B) D-**6** and (1*R*,2*R*)-**9** under stirring in a mixed solvent of water and THF, v/v 95:5 (concentration of all compounds is 1.0×10^{-3} M).

also gave single-hole nanospheres. Mixtures of D-**6** with (1*R*,2*S*)-**7** or (1*S*,2*R*)-**7** gave nanospheres with a larger hole. Exceptionally, even a suspension of D-**6** itself without amine in water and THF formed single-hole nanospheres (Figure 6C). The suspension of single-hole nanospheres prepared by the mixture of D-**6** with amine **7** or **9** was very stable. Precipitates and phase separation were not observed even after 3 months at room temperature. The aged suspension actually exhibited more consistent single-hole nanospheres because shallow or small holes on some nanospheres became deeper or larger (image D compared with image A of Figure 6). Due to the double bond at the end of undecenamide group of **6**, these single-hole nanospheres could be immobilized by suspension polymerization, if this is desired.

As shown in Figures 7, A and B, the TEM image also confirmed the existence of a single hole in the surface of the nanospheres. The size of the hole in the D-**6** and (1*R*,2*R*)-**9** nanospheres was significantly larger than that of D-**1** and (1*R*,2*R*)-**9** which agrees with the results from the FE-SEM images. In addition, a round shell could clearly be observed inside the nanosphere, indicating that the nanospheres were hollow.

The suspension of the nanofibers from the mixture of D-**1** and (1*S*,2*R*)-**7** and that of the nanospheres from D-**1** and (1*R*,2*S*)-**7** in a mixed solvent of water and ethanol, v/v 9:1,

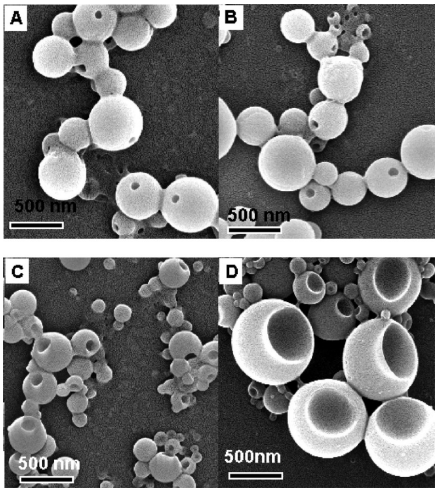

FIGURE 8. FE-SEM images of suspension of D-**6** and (1*R*,2*R*)-**9** in water/THF, v/v (A) 80:20; (B) 85:15; (C) 90:10 under no stirring ([D-**6**] = [(1*R*,2*R*)-**9**] = 1.0×10^{-3} M). (D) Suspension of D-**6** and (1*R*,2*R*)-**9** in H_2O/THF by evaporating THF from volume ratio 1:1 to about 95:5.

were investigated by dynamic light scattering (DLS). It was disclosed that the former suspension had particles with a mean diameter of 2996 nm, while the latter one had a mean diameter of 440 nm. The very large diameter demonstrates that the aggregates in the former suspension are probably nanofibers. The mean diameters of nanospheres with a hole from mixture of D-**1**, D-**2**, D-**3**, D-**4**, D-**5**, or D-**6** with (1*R*,2*R*)-**9** in a mixed solvent of water and THF, v/v 95:5, were 228, 220, 284, 241, 244, and 249 nm respectively, measured by the DLS.

The size of the hole on the surface of the nanospheres could be controlled by the volume ratio of water and THF. As shown in Figure 8, A−C, and Figure 6A, the diameter of the largest hole that could be seen increased from 70, 110, and 150 to 200 nm when the ratio of water and THF increased from 80:20, 80:15 and 90:10 to 95:5, respectively. The mean diameter of the holes is 60, 100, 140, and 180 nm, respectively. When the suspension of D-**6** and (1*R*,2*R*)-**9** in H_2O/THF (about 95:5) was prepared by evaporating THF from the solution of D-**6** and (1*R*,2*R*)-**9** in H_2O/THF 1:1, the diameter of the hole in the resultant spheres reached 500 nm, which made the sphere look more like a bowl (Figure 8D). The mean diameter of the holes is 250 nm.

In addition, nanospheres with no hole could be prepared by adding water without stirring to mixtures of D-**1**, D-**2**, D-**3**, D-**4**, or D-**5** with (1*R*,2*R*)-**9**. After standing for about 4 days at room temperature, holes also appeared in these nanospheres. When water and ethanol was used instead of water and THF, with or without stirring or after standing, only closed nanospheres were seen. The aged suspension of D-**6** and (1*R*,2*R*)-**9** exhibited better single-hole nanospheres after one month at room temperature (Figure 6D compared with Figure 6A). Some smaller nanospheres were encapsulated in the hole of the larger nanospheres (Figures S24 and S25, SI), and some of nanospheres had more than one hole (Figure S26, SI). All the above results demonstrated that the hole was not formed during the aggregation but appeared after the nanospheres had been produced. All the holes were smooth, and the surface around the hole seemed to be bent toward the interior. In addition, some of the holes were quite shallow. This implies the

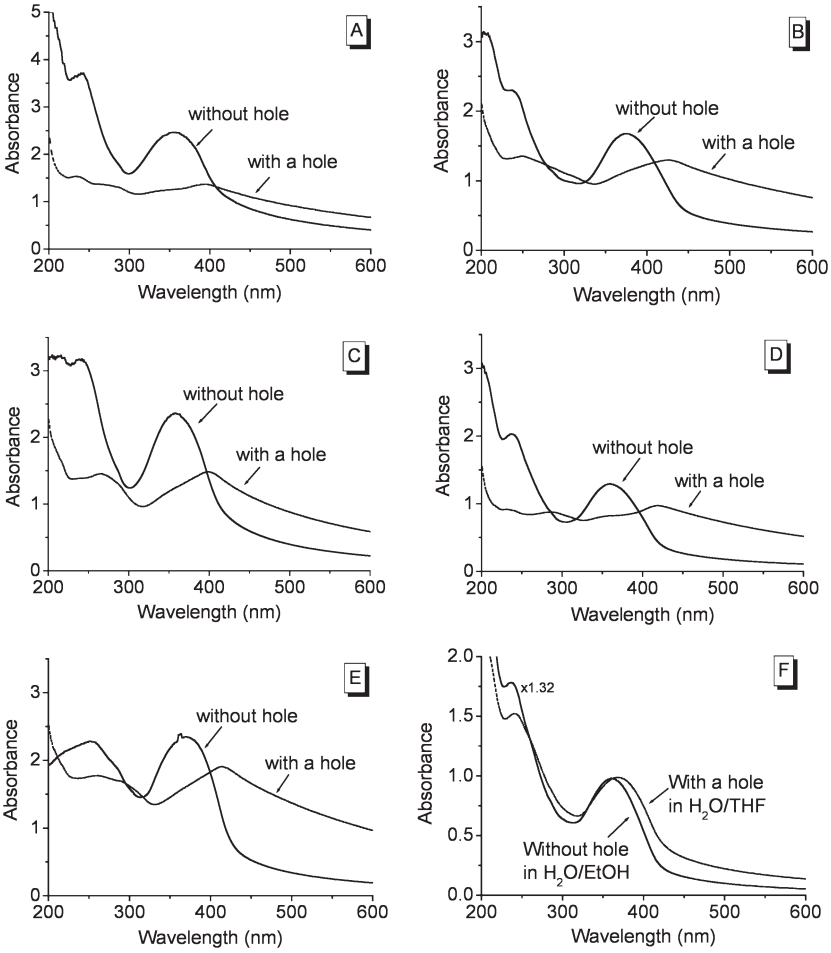

FIGURE 9. Absorption spectra of mixture of (A) D-**1** and (1*R*,2*R*)-**9**; (B) D-**2** and (1*R*,2*R*)-**9**; (C) D-**3** and (1*R*,2*R*)-**9**; (D) D-**4** and (1*R*,2*R*)-**9**; (E) D-**5** and (1*R*,2*R*)-**9** in a mixed solvent of water and THF, v/v 95:5. (F) Absorption spectra of D-**6** in the mixed solvent of H_2O/THF, v/v 95:5, and the mixed solvent of H_2O/ethanol, v/v 95:5.

hole was formed by etching or dissolution by the solvent starting from the exterior, not by the solvent flowing out of the interior of the nanosphere.[4,9,12] It has been reported that organic solid nanorods can be transformed into hollow nanotubes by a similar dissolution process.[17] Agitation and heat or prolonged standing allows the solvent to preferentially dissolve defects in the nanorod and gives a tubular result.[17] In our case, the formation of the hole occurs through a similar dissolution process. It is known that pores are produced at each vertex of the icosahedron formed by self-assembly of one fat acid and one quaternary ammonium base in order to minimize the curvature energy at the vertex.[18] Compared to nanorods or nanofibers, nanospheres have a more curved surface, and the production of a hole may reduce the bending energy.[18,19] Therefore, both the dissolution of defects and the relief of energy associated with bending are probably the driving forces in the production of a hole.

The bending energy could also be observed in the absorption and fluorescence spectra of the suspensions. In compounds from D-**1** to D-**6**, there are two phenyl groups and one cyano group connected by a double bond. If these groups are in the plane of the double bond, the compound will exhibit the longest λ_{max} in both the absorption and emission spectra. On the other hand, the emission intensity will tend to decrease when this conjugation is reduced. In a nanosphere, increases in the bending energy will cause these groups to twist and deviate from the plane of the double bond. This will lead to absorption and emission peaks at a shorter wavelength and in a weaker emission intensity. In nanofibers, these groups are more likely to conjugate into a double bond than in nanospheres, giving the nanofibers longer absorption and emission λ_{max} and stronger emission intensities. This agrees with the above observations (Table 1, Figures 2 and 4), demonstrating that the groups connected to the double bond in the D-**1**−D-**6** acids in the nanospheres are more twisted and less conjugated than those in nanofibers or nanorods.[20]

(17) (a) Jia, C.-J.; Sun, L.-D.; Yan, Z.-G.; You, L.-P.; Luo, F.; Han, X.-D.; Pang, Y.-C.; Zhang, Z.; Yan, C.-H. *Angew. Chem., Int. Ed.* **2005**, *44*, 4328–4333. (b) Zhang, X.; Zhang, X.; Shi, W.; Meng, X.; Lee, C.; Lee, S. *Angew. Chem., Int. Ed.* **2007**, *46*, 1525–1528.

(18) Dubois, M.; Deme, B.; Gulik-Krzywicki, T.; Dedieu, J.-C.; Vautrin, C.; Desert, S.; Perez, E.; Zemb, T. *Nature* **2001**, *411*, 672–675.

(19) (a) Fogden, A.; Daicic, J.; Kidane, A. *Colloids Surf., A* **1997**, *129−130*, 157–165. (b) Dubois, M.; Belloni, L.; Zemb, T.; Deme, B.; Gulik-Krzywicki, T. *Prog. Colloid Polym. Sci.* **2000**, *115*, 238–242.

(20) (a) Oelkrug, D.; Tompert, A.; Gierschner, J.; Egelhaaf, H.-J.; Hanack, M.; Hohloch, M.; Steinhuber, E. *J. Phys. Chem. B* **1998**, *102*, 1902–1907. (b) Kim, S.; Zheng, Q.; He, G. S.; Bharali, D. J.; Pudavar, H. E.; Baev, A.; Prasad, P. N. *Adv. Funct. Mater.* **2006**, *16*, 2317–2323.

(21) Shimizu, T.; Masuda, M.; Minamikawa, H. *Chem. Rev.* **2005**, *105* (4), 1401–1443.

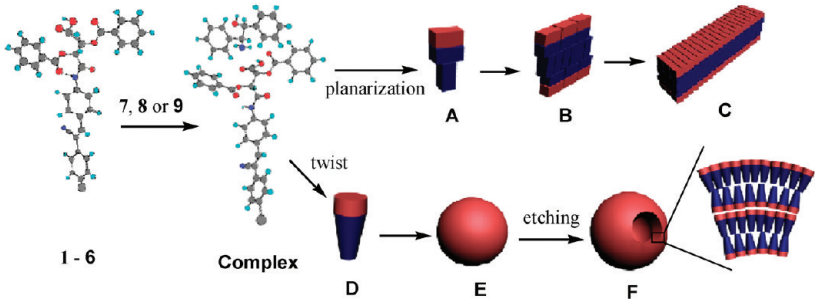

FIGURE 10. Schematic illustration for the formation of nanofibers, nanospheres, and hollow nanospheres with a hole.

The energy difference between the twisted and planar molecules is about 20 kJ mol^{-1} according to the relationship of energy and frequency of light wave ($E = h\nu$). It should mainly result from the bending energy at the surface of the nanospheres. A hole in the surface of a nanosphere would reduce the bending energy, causing the wavelength of the nanosphere to be longer than in a closed one. This effect can be seen in parts A−E of Figure 9. When water was added into mixtures D-**1**, D-**2**, D-**3**, D-**4**, or D-**5** with (1*R*,2*R*)-**9** in THF with stirring, conditions which led to nanospheres with a hole, the absorption λ_{max} of the resultant suspension was longer than that without stirring, which gave closed nanospheres. The difference between wavelengths of single-hole nanospheres and closed ones, $\Delta\lambda_{max}$, was 40 nm (400 vs 360 nm) for D-**1**, 50 nm (430 vs 380 nm) for D-**2**, 41 nm (404 vs 363 nm) for D-**3**, 56 nm (424 vs 368) for D-**4**, and 45 nm (424 vs 379 nm) for D-**5**. The mixture of D-**6** and (1*R*,2*R*)-**9** in a mixed solvent of water and THF only produced single-hole nanospheres, but the mixture in water and ethanol only afforded closed ones. It was also showed that the suspension of single-hole nanospheres had a longer wavelength of maximum absorption (373 nm) than that of closed ones (360 nm) (Figure 9E), although the maximum absorption of the solution of D-**6** and (1*R*,2*R*)-**9** in ethanol was longer than that in THF. Therefore the production of a hole reduces the bending energy by 12−43 kJ/mol. In addition, the emission intensity of single-hole nanospheres was always larger than that of nanospheres without a hole, and the emission maximum of the single-hole nanospheres was always at a longer wavelength than that of nanospheres without holes (Figure S29, SI).

A potential mechanism of the formation of a hole in the nanospheres and nanofibers is shown in Figure 10. Compounds **1**, **2**, **3**, **4**, **5**, and **6** are wedge shaped, and the complexes of these acids with amines **7**, **8**, or **9** are also wedge shaped (A and D).[20] If the molecule is more planar and conjugated, it will be like a T-shaped ruler A and can arrange in parallel, which will result in nanofibers C. If the molecule is more twisted and less conjugated, the molecule will be more of a circular cone (Figure 10D) which cannot be arranged in parallel but tends to form a circular arrangement. This leads to nanosphere as in Figure 10E. The complexes can be formed through Coulombic, hydrogen-bonding, $\pi-\pi$ stacking, and hydrophobic forces. The association constant K_a of L-**1** with (1*S*,2*R*)-**7** is 1.02×10^5 M^{-1} which is larger than that of L-**1** with (1*R*,2*S*)-**7** (8.98×10^3 M^{-1}).[16] This means that enantiomer (1*S*,2*R*)-**7** interacts more strongly with acid L-**1** than its enantiomer, which will drive the phenyl group connected to the double bond out of conjugation. Therefore, (1*S*,2*R*)-**7** leads to nanospheres, and (1*R*,2*S*)-**7** results in nanofibers upon

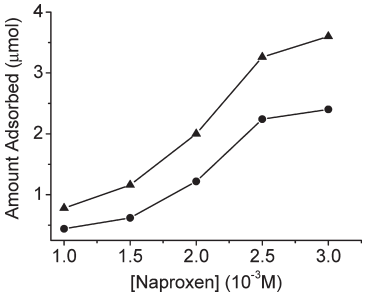

FIGURE 11. Amount of naproxen (μmol) adsorbed by the aggregates from 2 mL of suspension of D-**1** and (1*R*,2*R*)-**9** (1.0×10^{-3} M) changed with the concentration of naproxen. (▲) by nanospheres with a hole; (●) by nanospheres without hole.

interaction with L-**1**. In addition, chiral diamine **9** interacts more strongly with the acids, having a K_a with L-**1** greater than 10^6 M^{-1};[16] therefore, it tends to form nanospheres. Finally the nanosphere with a hole (Figure 10 F) is produced by solvent etching because of defects and reduction in the bending energy in the surface.

The nanospheres formed from a mixture of D-**1** and (1*R*,2*R*)-**9** were used to test the encapsulation of naproxen **10**. Naproxen, a nonsteroidal anti-inflammatory drug, is an α-aromatic propionic acid with a very low solubility in water. Hydrogen-bonding, $\pi-\pi$ interaction, and hydrophobic forces will cause naproxen to be included in the aggregates composed of D-**1** and (1*R*,2*R*)-**9** complex. Thus, 0.02 mL of 0.3 M naproxen in THF was added to 2 mL of a suspension of D-**1** and (1*R*,2*R*)-**9** (1.0×10^{-3} M) in water and THF (v/v 9:1) prepared with stirring, and the mixture of naproxen and the suspension was slowly stirred for 1 h at room temperature. Under similar conditions, naproxen was tested with the suspension of D-**1** and (1*R*,2*R*)-**9** in the same solvent when freshly prepared, without stirring. The residual naproxen was removed by centrifuge, and the clear solution was analyzed by fluorescence; 1.2×10^{-3} M of the naproxen remained in solution after interacting with the suspension prepared with stirring, but 1.8×10^{-3} M remained after interacting with the freshly prepared suspension without stirring. The same results were obtained in three repetitions of the test. This means that 2.4 μmol of naproxen was encapsulated by nanospheres without holes and 3.6 μmol was encapsulated by nanospheres with a hole. When the concentration of naproxen was varied from 1.0×10^{-3} M to 3.0×10^{-3} M, the amount of naproxen encapsulated by the nanospheres with a hole was always larger than by nanospheres without a hole (Figure 11). At the 3.0×10^{-3} M

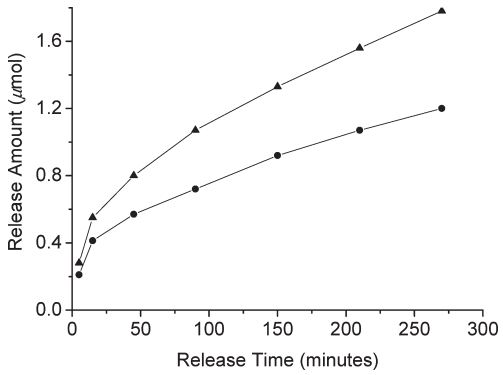

FIGURE 12. Release amount in water of naproxen (μmol) included in the aggregates from 2 mL of suspension of D-**1** and (1*R*,2*R*)-**9** (1.0×10^{-3} M) by adding 0.02 mL of 0.3 M naproxen changed with time. (▲) by nanospheres with a hole; (●) by nanospheres without hole.

concentration of naproxen, the hollow nanospheres with a hole could absorb 50% more naproxen than the closed nanospheres.

The release of naproxen in water from the aggregates was also investigated using the original conditions above. Upon centrifugation was removed 1.6 mL of supernatant from the above encapsulation test of a mixture of 0.02 mL of 0.3 M naproxen in THF and a 2 mL of suspension of D-**1** and (1*R*,2*R*)-**9** (1.0×10^{-3} M) in the mixed solvent of water and THF (v/v 9:1). Then 1.6 mL of distilled water was added into the residue and stirred at room temperature. The suspension was centrifuged again, and the supernatant was removed for analysis of naproxen. Again, 1.6 mL of distilled water was added for the next release test. This process was repeated with different stirring times. As shown in Figure 12, naproxen included in the nanospheres with a hole was released more quickly than from nanospheres without a hole. Moreover, the difference in the amount released by the nanospheres with a hole versus that by nanospheres without a hole increased with increasing time. This result demonstrates that nanospheres with a hole not only could release more included naproxen but also had a higher release speed than nanospheres without a hole.

Conclusion

In conclusion, chiral AIE acids have for the first time enantioselectively self-assembled with the two enantiomers of chiral amines in mixed solvents to form either nanofibers or nanospheres. The nanofibers exhibited a stronger emission intensity and longer absorption and emission λ_{max} than the nanospheres. In water and THF, the resultant nanospheres produced a single hole because of the dissolution of defects and reduction in the bending energy. The single-hole nanospheres displayed both higher uptake capacity and larger release speed for the drug naproxen than the closed ones. The decrease in the energy associated with bending in the surface by hole formation was directly observed. These findings provide a new approach to adjust the fluorescent properties of AIE molecules and the preparation of organic single-hole hollow nanospheres. Other applications of hollow nanospheres with a hole, for example as a template for the preparation of inorganic nanospheres with a hole, are under investigation.

Experimental Section

Materials. All reagents and solvents were of chemically pure (CP) grade or analytical reagent (AR) grade and were used as received. D- and L-2,3-dibenzoyltartaric anhydride were homemade by the reaction of D- and L-tartaric acid with benzoyl chloride, respectively, in the presence of a catalytic amount of $FeCl_3 \cdot 6H_2O$.

Measurements. ^{1}H NMR and ^{13}C NMR spectra were measured on a 400 MHz spectrometer at 298 K in $CDCl_3$. Fluorescent emission spectra were collected on a fluorophotometer at 298 K. Absorption spectra were recorded on a UV−vis spectrophotometer. The mass spectrum was measured on a FTMS instrument. The powder X-ray diffraction (XRD) pattern was measured on a diffraction instrument. Dynamic light scattering (DLC) was measured on a particle size analyzer. Infrared spectra were recorded on a spectrometer.

Field emission scanning electron microscopy (FE-SEM) images were taken on an electron microscope operating at 5 kV or 10 kV. The suspension of a sample was dropped onto a slide and air dried. Transmission electron micrographs (TEM) were recorded on an electron microscope at 200 kV. The suspension was dropped onto a copper grid covered with a thin carbon film on filter paper and air dried.

Typical Self-Assembly of the Hollow Nanospheres with a Hole. D-**1** (0.002 mmol) and (1*R*,2*R*)-**9** (0.002 mmol) were dissolved in THF (0.2 mL) at room temperature. The solution was diluted to 2 mL with deionized water under stirring, and the resultant suspension continued stirring for 0.5 h. The suspension was directly used for analysis. Instead, the hollow nanospheres with a hole were collected by centrifuging the suspension.

Synthesis of Phenylacrylonitrile Tartaric Acids 1−6. Synthesis of **2**−**6** was similar to that of **1** which has been reported.[16]

Synthesis of Compound D-2. To a flask was added *N*-acetyl-*p*-aminocinnamonitrile (0.01 mol), D-2,3-dibenzoyltartaric acid anhydride (3.7 g, 0.011 mol), and dry THF (30 mL). The mixture was stirred at room temperature for 24 h, evaporated to about 2 mL, into which methanol or ethanol was poured, and the resultant yellow solid was collected by filtering (3.6 g, 58%). Mp 235−236 °C; $[\alpha]^{20}_D$ +20 (*c*, 1.0, THF); IR (kBr) *ν* 3512, 3307, 3108, 3065, 2217, 1739, 1713, 1668, 1602,1 525, 1452, 1414 cm^{-1}; ^{1}H NMR (400 MHz, DMSO-d_6) *δ* 10.84 (s, 1H), 10.17 (s, 1H), 8.05 (q, *J* = 7.6 Hz, 4H), 7.88−7.84 (m, 4H), 7.76 (s, 1H), 7.70−7.84 (m, 6H), 7.63−7.89 (m, 4H), 6.06, 5.97 (2d, *J* = 36 Hz, 2H), 2.08 (s, 3H); ^{13}C NMR (100 MHz, DMSO-d_6) *δ* 168.5, 167.3, 164.9, 164.8, 163.6, 140.3, 140.1, 139.7, 134.1, 130.0, 129.5, 129.4, 129.0, 128.6, 128.5, 128.3, 126.1, 119.6, 119.1, 118.1, 108.4, 72.8, 71.5, 23.5; ESI$^-$ MS *m*/*z* calcd for $C_{35}H_{27}N_3O_8$ 617 [M], found 616.2 [(M − 1)]$^-$. Anal. Calcd for for $C_{35}H_{27}N_3O_8$: C, 68.07; H, 4.41; N, 6.80. Found: C, 67.87; H, 4.37; N, 6.72.

Synthesis of Compound D-3. The synthetic procedure is similar to that of D-**2**; yield, 80%. Mp 117−119 °C; $[\alpha]^{20}_D$ +19 (*c*, 1.0, THF); IR (kBr) *ν* 3288, 3118, 3067, 2925, 2221, 1731, 1599, 1533, 1493, 1452, 1417 cm^{-1}; ^{1}H NMR (400 MHz, DMSO-d_6) *δ* 10.85 (s, 1H), 8.04 (q, *J* = 7.2 Hz, 4H), 7.99 (s, 1H), 7.91 (d, *J* = 8.4 Hz, 2H), 7.77−7.70 (m, 6H), 7.64−7.56 (m, 6H), 6.05, 5.96 (2d, *J* = 36 Hz, 2H); ^{13}C NMR (100 MHz, DMSO-d_6) *δ* 167.2, 164.8, 164.7, 163.6, 142.7, 140.1, 134.0, 133.9, 133.6, 130.2, 129.4, 129.3, 129.1, 129.0, 128.9, 128.6, 128.5, 127.3, 119.5, 117.7, 107.4, 72.8, 71.5; ESI$^-$ MS *m*/*z* calcd for $C_{33}H_{23}N_2O_7Cl$ 594.5 [M], found 593.3 [(M − 1)]$^-$. Anal. Calcd for for $C_{33}H_{23}N_2O_7Cl$: C, 66.61; H, 3.90; N, 4.71. Found: C, 66.58; H, 3.92; N, 4.68.

Synthesis of Compound D-4. The synthetic procedure is similar to that of D-**2**; yield, 56%. Mp 196−197 °C; $[\alpha]_D^{20}$ +44 (*c* 1.0, THF); IR (KBr) *ν* 3468, 3113, 2922, 2852, 1737, 1718, 1602, 1521 cm^{-1}; ^{1}H NMR (400 MHz, DMSO-d_6) *δ* 13.97 (br s, 1H,

COO*H*), 10.87 (s, 1H, N*H*), 8.40−7.40 (m, 22H, Ar*H*), 7.18 (s, 1H, =C*H*), 6.06 (s, 1H, C*H*), 5.96 (s, 1H, C*H*); ^{13}C NMR (100 MHz, DMSO-d_6) δ 167.2, 164.8, 164.7, 163.6, 142.2, 141.6, 140.0, 134.2, 134.0, 133.9, 132.7, 130.1, 129.4, 129.3, 129.1, 128.9, 128.6, 128.5, 128.4, 126.6, 126.4, 125.8, 119.5, 117.9, 108.0, 79.1, 72.8, 71.5; ESI$^-$ MS *m*/*z* calcd for $C_{37}H_{26}N_2O_7S$ 642 [M], found 641.0 $[(M-1)]^-$. Anal. Calcd for for $C_{37}H_{26}N_2O_7S$: C, 69.15; H, 4.08; N, 4.36. Found: C, 69.33; H, 4.20; N, 4.39.

Synthesis of Compound D-5. The synthetic procedure is similar to that of D-**2**; yield, 82%. Mp 216−218 °C; $[\alpha]^{20}_D$ +20 (*c*, 1.0, THF); IR (kBr) ν 3516, 3306, 3064, 2214, 1739, 1715, 1671, 1654, 1600, 1522, 1452, 1414 cm^{-1}; ^{1}H NMR (400 MHz, DMSO-d_6) δ 10.84 (s,1H), 10.47 (s, 1H), 8.05 (q, J = 7.6 Hz, 4H),7.98 (d, J = 7.2 Hz, 2H), 7.95 (s, 1H), 7.93−7.90 (m, 2H), 7.72 (q, J = 8.4 Hz, 4H), 7.65−7.53 (m, 6H), 6.06, 5.96 (2d, J = 40 Hz, 2H); ^{13}C NMR (100 MHz, DMSO-d_6) δ 167.3, 165.5, 164.9, 164.8, 163.6, 140.6, 140.0, 139.8, 134.7, 134.0, 130.0, 129.5, 129.4, 129.0, 128.9, 128.6, 128.5, 128.4, 127.7, 126.0, 120.5, 119.6, 72.8, 71.5; ESI$^-$ MS *m*/*z* calcd for $C_{40}H_{29}N_3O_8$ 679 [M], found 678.2 $[(M-1)]^-$. Anal. Calcd for for $C_{40}H_{29}N_3O_8$: C, 70.69; H, 4.30; N, 6.18. Found: C, 70.52; H, 4.37; N, 6.15.

Synthesis of Compound D-6. The synthetic procedure is similar to that of D-**2** except D-**6** was purified by recrystallization from methanol and water; yield, 74%. Mp 125−128; $[\alpha]^{20}_D$ +17 (*c*, 1.0, THF); IR (kBr) ν 3324, 3109, 3066, 2926, 2854, 2214, 1730, 1670, 1599, 1529, 1452, 1413; ^{1}H NMR (400 MHz, DMSO-d_6) δ 10.82 (s, 1H), 10.08 (s, 1H), 8.04 (q, J = 7.6 Hz, 6H), 7.88−7.84 (m, 4H), 7.74−7.55 (m, 9H), 6.03, 5.96 (2d, J = 28 Hz, 2H), 5.82−5.75 (m, 1H), 5.01−4.91 (m, 2H), 2.32 (t, J = 7.2 Hz, 2H), 2.01 (m, 2H), 1.59 (m, 2H), 1.27(m, 10H); ^{13}C NMR (100 MHz, DMSO-d_6) δ 171.5, 167.3, 164.9, 164.7, 163.7, 140.2, 140.0, 139.7, 138.7, 134.0, 133.9, 129.8, 129.4, 129.3, 128.9, 1286, 128.2, 126.0, 119.5, 119.1, 118.0, 114.5, 108.3, 72.9, 71.7, 36.3, 33.1, 28.6, 28.5, 28.4, 28.1, 24.9; ESI$^-$ MS *m*/*z* calcd for $C_{44}H_{43}N_3O_8$ 741 [M], found 740.4 $[(M-1)]^-$. Anal. Calcd for for $C_{44}H_{43}N_3O_8$: C, 71.24; H, 5.84; N, 5.66. Found: C, 71.13; H, 5.79; N, 5.60.

Acknowledgment. This research work was supported by National Natural Science Foundation of China (No. 20872040 and 21072067), the Fundamental Research Funds for the Central Universities (HUST: No. 2010ZD007) and the Analytical and Testing Centre at Huazhong University of Science and Technology.

Supporting Information Available: Experimental details, spectra, and more images. This material is available free of charge via the Internet at http://pubs.acs.org.